


## Article

# Design and Testing of Bionic-Feature-Based 3D-Printed Flexible End-Effectors for Picking Horn Peppers

Lexing Deng, Tianyu Liu \* , Ping Jiang, Aolin Qi, Yuchen He, Yujie Li, Mingqin Yang and Xin Deng

College of Mechanical and Electrical Engineering, Hunan Agricultural University, Changsha 410128, China

\* Correspondence: liutianyu@hunau.edu.cn

**Abstract:** To solve the problems of poor adaptability and large sizes of pepper harvesting machinery in facility agriculture to enhance the efficiency and quality of pepper harvesting and ultimately boost farmers' income, several flexible end-effectors were designed. These end-effectors were tailored to the unique morphologies of horn peppers, drawing inspiration from biomimicry. Subsequently, we conducted experimental verification to validate their performance. Four biological features, namely, the outer contours of a *Vicia faba* L. fruit, an *Abelmoschus esculentus* fruit, the upper jaw of a *Lucanidae*, and a *Procambarus clarkii* claw, were selected and designed using 3D software. In order to ascertain the structural viability and establish the initial design framework for the test end-effector, a simulation analysis to evaluate the strength and deformation of the flexible end-effector under various pepper-picking conditions was conducted. PLA material and 3D printing technology were used to create the end-effector, and, together with the mobile robotic arm platform ROSMASTER X3 PLUS, they were used to build a test prototype; a pepper tensile test was performed to pre-determine the reasonableness of the picking program, and then a prototype was created for the actual picking of the peppers to compare the picking effectiveness of several types of flexible end-effectors. In six experiments, each flexible end was harvested for 120 horn peppers. The *Vicia faba* L. flexible end-effector had the lowest average breakage rate. The average breakage rate was 1.7%. At the same time, it had the lowest average drop rate. The average drop rate was 3.3%. The test results indicated that the flexible end-effector that emulated the outer contour characteristics of the *Vicia faba* L. fruit demonstrated the most favorable outcomes. This design exhibited high working efficiency and the lowest rates of fruit breakage and fruit drops, surpassing both the artificial and traditional machine picking methods and effectively fulfilling the requirements for pepper-picking operations in facility agriculture.

**Keywords:** pepper harvesting; biomimicry; structural design; agricultural robotics; adaptive adjustment



**Citation:** Deng, L.; Liu, T.; Jiang, P.; Qi, A.; He, Y.; Li, Y.; Yang, M.; Deng, X. Design and Testing of Bionic-Feature-Based 3D-Printed Flexible End-Effectors for Picking Horn Peppers. *Agronomy* **2023**, *13*, 2231. <https://doi.org/10.3390/agronomy13092231>

Academic Editors: Baohua Zhang and Yongliang Qiao

Received: 6 August 2023

Revised: 22 August 2023

Accepted: 23 August 2023

Published: 26 August 2023



**Copyright:** © 2023 by the authors. Licensee MDPI, Basel, Switzerland. This article is an open access article distributed under the terms and conditions of the Creative Commons Attribution (CC BY) license (<https://creativecommons.org/licenses/by/4.0/>).

## 1. Introduction

Peppers, widely acclaimed as a popular condiment and ingredient worldwide, also hold significant economic importance as a cash crop, with global exports exceeding 10 percent of the total vegetable and fruit exports, creating millions of jobs and contributing to economic development [1]. In recent years, numerous countries around the world have been actively supporting the modernization of facility-based agriculture in the pepper industry [2]. Facility agriculture offers a viable solution to reduce the industry's reliance on natural conditions, thus expanding the development possibilities across different locations and time frames. The key areas of focus include pepper variety cultivation, cold chain logistics for warehousing and preservation, and advanced processing techniques, particularly in the realm of intelligent harvesting machinery for the peppers [3]. The pepper-picking process in facility agriculture faces considerable complexity and numerous challenges. The complexities of the picking process, coupled with the propensity of pepper fruits to break easily, a short picking period, labor-intensive operations, and unfavorable picking

conditions, significantly hinder the progress of the pepper industry and negatively impact the economic returns of pepper farmers [4].

Bionic design involves the refining of design concepts by simulating the forms, principles, or fundamental features found in biological systems in nature. It serves as a significant source of inspiration for a modeling design [5], and many scholars have optimized the shape of robot end-effectors through this design method.

Jian Li et al. introduced a soft-limb device inspired by the entanglement behavior observed in vines and plants. The device incorporated symmetric chambers in its kinematics, enabling the entanglement of the vines and plants through coupling motions, either under different or the same pressure conditions [6]. Alkin Yilmaz Akter et al. introduced giant anteater and American badger forepaw shapes and curves into a bucket design, and the computer-aided static analysis showed that the design was able to reduce the total deformation during operation and provide more excavation stress to the soil compared with the standard bucket teeth [7]. Haiyang Jiang et al. took inspiration from the tooth contour observed in the rigid claw of the Boston lobster. They performed an initial imitation, explored the design parameterization, and developed a bionic parameterization of the original tooth contour on the lobster's claw. This process resulted in the creation of seven bionic finger surface designs. Subsequent underwater experiments validated that the bionic finger surface design significantly enhanced the success rate of grasping [8]. Fuwen Hu et al. created a new type of plant-inspired soft robotic gripper by reconstructing and simulating the leaf structure and head formation mechanism of cabbage and successfully conducted grasping experiments [9].

Many developed countries have begun early research on pepper harvesting machinery for facility agriculture, and, currently, the research results are more mature, more widely used, and better promoted. Shivaji Bachche et al. presented a design for a five-degree-of-freedom robotic arm gripper and cutting system for pepper harvesting. This design consisted of two parallel jaws mounted on a gear and worked with the help of servo motors. Comparative experiments showed that this equipment had a good harvesting performance [10]. A robotic SWEEPER for harvesting pepper fruits in a greenhouse was designed by Boaz Arad et al. This robotic system consisted of a six-degree-of-freedom industrial arm equipped with a specially designed end-effector, RGB-D video camera, and programmable logic controller, among others. Experiments have demonstrated that this robotic manipulator was able to operate at higher speeds and had a higher success rate in harvesting [11]. A robot for the autonomous harvesting of peppers in facility agriculture was evaluated by C. Wouter Bac et al. Stem dependence was assessed by comparing the harvesting results of two end-effector shapes (fin shape and lip shape) to determine the performance contribution of the gripping posture [12].

Most developing countries began researching pepper-harvesting machinery relatively late and are basically at the stage of manual harvesting or semi-mechanized harvesting. Zhengtong Ning et al. presented an algorithm designed to recognize peppers and then planned a strategic harvesting sequence. This algorithm has proven to be effective in enhancing the operational efficiency of the robots engaged in multi-objective pepper-picking within intricate orchards characterized by intensive planting. Additionally, it helped prevent potential collision damage during the harvesting process [13]. Lei Jin et al. designed the working principle of a new type of picking device for pepper harvesters. The optimal rotational speed and translational speed of the spring tines were determined by establishing the spring tine trajectory equations, and the optimal height of the passive roller was determined from the characteristic parameters of the peppers. Using these optimization parameters, the pepper harvester was modified. The experimental results showed that these optimization parameters could help accelerate the improvement, design, and development of the pepper harvester [14]. Yihan Wang et al. developed a perceptual model and improved upon it by proposing a cross-task feature enhancement (CTFE) strategy, which, in turn, utilized multitask relationships. This model could assist pepper robots in maintaining robust perception in unstructured environments to help in picking the fruits [15]. A number

of algorithms related to deep learning and adaptive tuning are driving the development of smart agricultural machinery [16–19].

However, the current research has some limitations: (1) Most of the machinery operates in a rough manner, destructively harvesting the trees, and the harvested peppers are easily damaged and contain high rates of impurities [20]. (2) The design of the end-effector of the harvesting mechanical arm is not adapted to the shape characteristics of the different types of peppers, and it is not possible to obtain higher harvesting efficiency and quality. (3) A considerable concern of the harvesting machinery is its large-volume design and its associated environmental impact, and it does not fully consider the applicability of facility agriculture in the harvesting scenario.

In order to solve the above limitations, we devised multiple variations in flexible end-effectors in facility agriculture that were tailored specifically to the horn pepper's unique shape. Leveraging the ROSMASTER X3 PLUS mobile robotic arm platform, we achieved an efficient and low-loss harvesting of the peppers. Four biological features were selected, namely, the outer contours of a *Vicia faba* L. (broad bean or fava bean) fruit, the *Abelmoschus esculentus* (okra) fruit, the upper jaw of a *Lucanidae* (spade beetle or stag beetle) specimen, and a *Procambarus clarkii* (crayfish or lobster) claw. SolidWorks was used to carry out the design of the shape-mimicking structure [21]. The feasibility of the four end-effector structures was confirmed through finite element analysis, which was used to examine their strengths and deformations under various picking scenarios. As a result, the imitation of the outer contour of *Vicia faba* L. was preliminarily determined as the optimal design; the reasonableness of the picking scheme was pre-determined through the pepper tensile test; and the flexible picking end-effector was fabricated by using PLA material and 3D printing technology [22]. Through field trials to compare the pepper-picking ability of the flexible end-effectors with different bionic characteristics and the subsequent analyses, the results showed that the broad bean characteristics for a flexible end-effector had the best effect, with high efficiency and the lowest fruit-breakage and drop rates; this end-effector performed significantly better than the manual and traditional machine picking and could well meet the requirements of pepper harvesting in facility agriculture.

In summary, the main contributions of this paper are as follows: (1) On the basis of the bionic features, a flexible end-effector for pepper harvesting with bionic broad bean fruit outer contour features was designed for the characteristics of horn peppers, which was able to achieve a higher work efficiency and lower fruit-breakage and fruit-drop rates. (2) A small and lightweight pepper harvesting machine was developed based on the ROSMASTER X3 PLUS robot, which was particularly suitable for the pepper-harvesting scenario in facility agriculture. (3) This study innovatively applied the principle of bionics to the style and design of a flexible end-effector for better pepper-harvesting effectiveness in facility agriculture, and it can serve as a reference for the design of pepper-harvesting equipment in facility agriculture in the future.

## 2. Bionic Design

Capsicum is an annual herbaceous plant of the genus *Capsicum* in the family Solanaceae and can be categorized according to the shape of the fruit as horn peppers, thread-like peppers, lantern peppers, or cherry peppers, etc., as shown in Figure 1. Among them, the horn pepper has a cone-shaped fruit, with a crisp taste, moderate spiciness, thin skin, thick flesh, transportation resistance, high yield, and other advantages. There is a wide demand and market all over the world for this pepper, and it is one of the key cultivars to be developed and cultivated in the pepper industry. In order to improve the efficiency and quality of pepper harvesting, this paper proposes a flexible end-effector styling design for the bullhorn pepper.

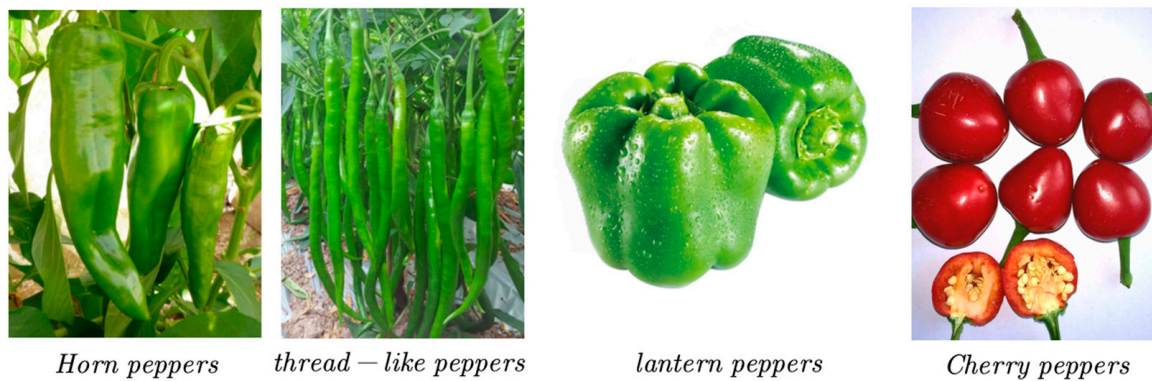


**Figure 1.** Different shapes of pepper varieties.

The “biologization” aspect is an important part of biomimetic design. By looking to nature for “How do organisms fulfill specific functions?”, transform the design problem into a biological problem. Further generate the solution model with functional keywords. Finally, retrieve from the biological knowledge base and match the biological prototype to realize the design solution to lay the foundation, as shown in Figure 2.

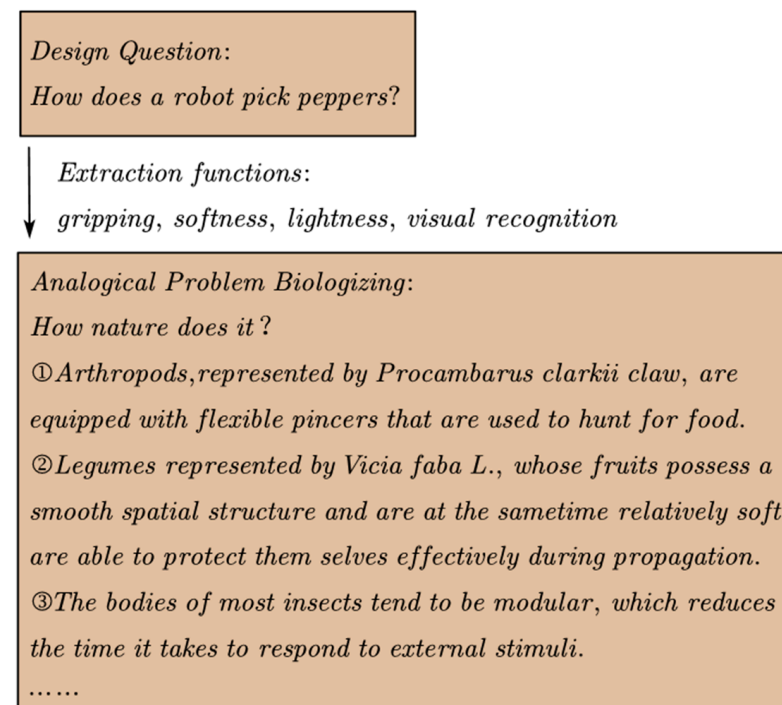


**Figure 2.** A model for solving biochemical problems.

Based on the above thinking, we selected four types of bionic organisms for this study: fava beans, okra, stag beetles, and lobsters. The bionic creature modeling is depicted in Figure 3. Establishing bionic mapping relationships is an important part of bionic design. The characteristic elements of these bionic entities were extracted based on the existing end-effector modeling of the pepper-harvesting robotic arm. This allowed for the establishment of a mapping relationship between the flexible end-effector modeling features and the features of the selected bionic organisms. Subsequently, this mapping was applied to the end-effector modeling of the four chosen organisms [23]. The extraction and evolution of the bionic features are illustrated in Figure 4.

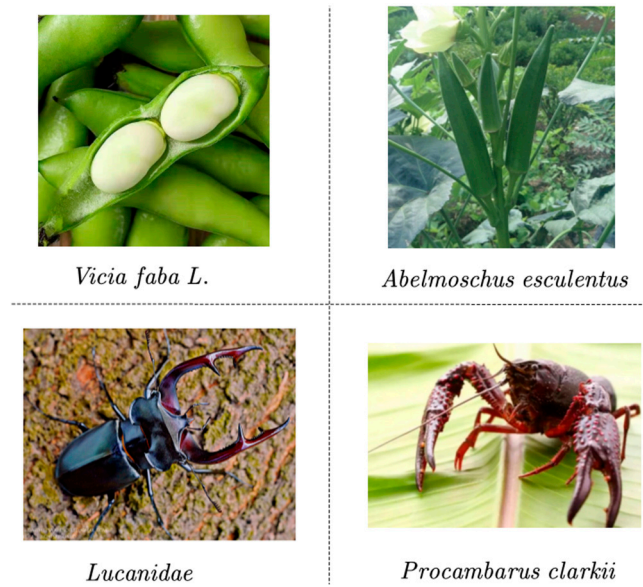


Figure 3. Bionic creature shapes used in this study.

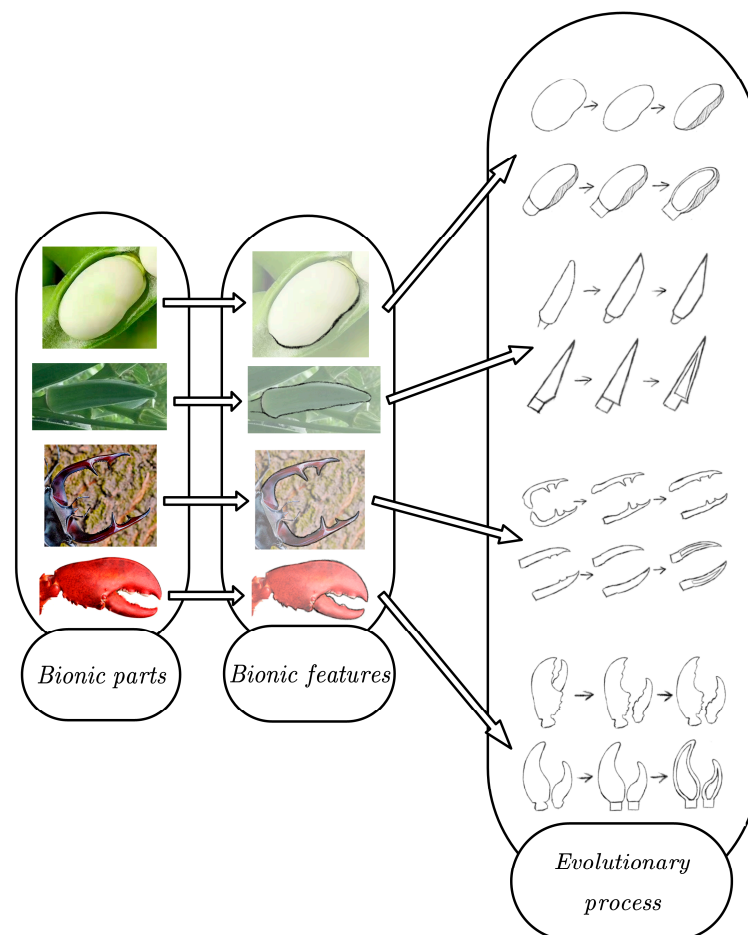
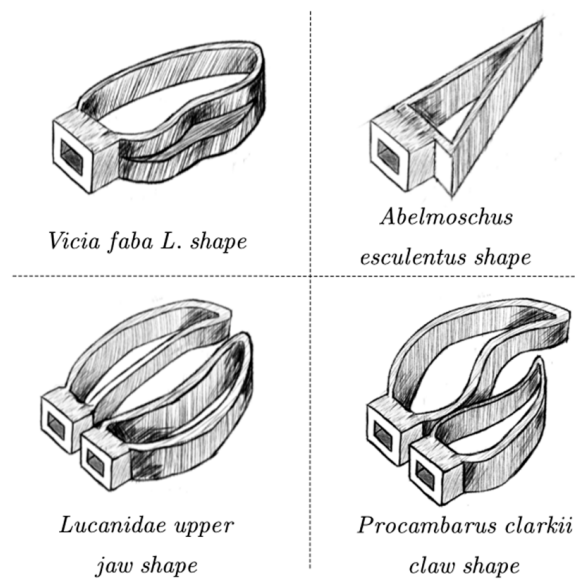


Figure 4. Extraction and evolution of bionic features.

By extrapolating the characteristic elements, four different flexible end-effector shapes for the peppers were ultimately designed. The schematic diagram of the flexible end-effector modeling is shown in Figure 5.



**Figure 5.** Schematic diagram of flexible end-effector shapes.

### 3. Harvesting Program Determination

#### 3.1. Tensile Testing and Parameter Measurement of Peppers

The working scheme of the flexible end-effectors designed in this study was as follows: The flexible end-effector was connected to the robotic picking arm through the clamping linkage parts. During the working time, the movement of the clamping linkage parts was driven by the servo on the robotic arm to activate the flexible end-effector to clamp the peppers. The flexible end was pulled slowly downward with the robotic arm. The pulling distance was roughly 15 cm; it was accompanied by a slow oscillation with an angular velocity of  $\frac{2\pi}{3}$  rad/s. Separation of the pepper from the tree could be achieved by the above actions (no need to repeat). The schematic diagram of the work process is shown in Figure 6.

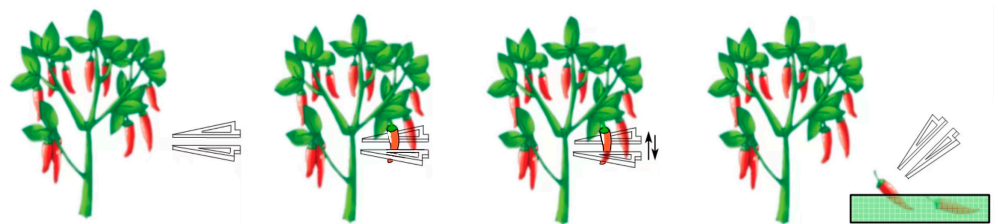


**Figure 6.** Schematic diagram of the work process.

Usually, peppers are harvested with the peduncle portion retained to maintain their freshness and improve their storage time [24]. In order to investigate the reasonableness of the above working scheme, it was necessary to determine whether the separation of the fruit stalk from the tree could be achieved by shaking the peppers during picking without destroying their integrity. In this study, we designed a pepper tensile resistance experiment: (1) The experiment used a dynamometer to connect the peppers that had not yet been picked; the strengths of the fruit stalks that were still attached to the tree were measured (in Newtons, N) by manually pulling on the dynamometer, and this value was denoted by  $F_1$ . (2) At the end-effector of experiment 1, for each pepper sample, the strength of the fruit-stem connection was measured again by pulling the dynamometer and the fruit stalk with both hands, and this was denoted as  $F_2$ .

This experiment was carried out in June 2023 at the research base of Hunan Agricultural University in Changsha, Hunan Province, China. The experimental variety was the ox horn pepper variety Xiangyan No. 15. At this period, the peppers had reached maturity.

The fruits took on the characteristic greenish-red color of the variety and were moderately hard. The force meter, a 10 N pointer push–pull force meter with a load index value of 0.05 N and an error of 1%, was selected from Dongguan ZHIQU Precision Instrument Co., Ltd., Eidelberg, NK (Dongguan, China). An example of the force meter is shown in Figure 7. Six well-grown pepper trees were randomly selected for the experiment, and one fresh, pest-free, surface-grown pepper sample was randomly selected from each tree for the two experiments described above. The connection method was as follows: The large mouth of the funnel-shaped net was wrapped around 2/3 of the body of the pepper fruit from bottom to top; it was wrapped for approximately several cycles with adhesive tape with a width of 2 cm. This was similar to the width of the flexible end-effector. The experiment used the force generated by the deformation of the tape to simulate the clamping force generated by the flexible end-effector during the experiment. The force-measuring instrument was connected to the small mouth of the screen through the hook adapter. During the experiment, if damage was caused to the trunk or branches due to separation of the chili peppers, the chili peppers were considered to be broken, and the measurements were not counted as valid data for the tensile test. This was because it fell under the category of harvesting impurities, did not affect the quality of the chili, and had a low probability of occurring. The schematic diagram of the measurement method is shown in Figure 8, and the data of the pepper tensile resistance experiments are shown in Table 1.



Figure 7. Dynamometer device used in the study.



Experiment 1



Experiment 2

Figure 8. Schematic diagram of the measurement method.

**Table 1.** Pepper tensile test data.

Separating Force	Serial Number	1	2	3	4	5	6	Average Value	Mean Square Deviation
	$F_1$		2.88	2.21	1.15	2.41	3.11	2.66	2.40
$F_2$		9.57	8.49	9.20	7.25	8.56	9.87	8.82	0.84

As seen from the experimental data in Table 1, in the six sets of experiments, the  $F_1$  values were always smaller than the  $F_2$  values, and a large gap was maintained within each pair of data. Meanwhile,  $F_1$  had the mean square deviation of 0.39, and  $F_2$  had the mean square deviation of 0.84. This indicated that the degree of variation in the data points relative to the mean was small, the data were relatively clustered around the mean, and the experiment was more credible. Therefore, the harvesting scheme proposed in this paper accomplished not only the separation of the fruit from the tree but also ensured the integrity of the fruit, which was in line with the real demands of pepper harvesting.

In order to further determine the design parameters of the four flexible end-effectors with bionic characteristics, the maximum diameter and weight of the fruiting bodies of six samples of peppers picked for the experiment were measured. To ensure the accuracy of the measurement data, three measurements were used to obtain the average value for each sample measurement. The parameters of the sample peppers are shown in Table 2.

**Table 2.** Sample pepper parameters.

Parameters	Sample Number	1	2	3	4	5	6	Average Value	Mean Square Deviation
	Maximum thickness of pericarp (mm)		3.2	3.4	3.0	4.0	2.9	3.5	3.3
Maximum diameter of fruiting body (mm)		24.2	24.3	26.0	20.8	25.2	21.3	23.7	1.93
Fruiting body length (cm)		13.8	15.2	15.8	16.1	16.2	14.2	15.2	0.93
Sample mass (g)		35	42	46	52	48	37	43.3	1.49

### 3.2. Determination of Flexible End-Effector Parameters

$F_1$  and  $F_2$  are important factors affecting the design of the flexible end-effector. Assuming that the flexible end-effector grasps the pepper and then shakes it without the end and the pepper sliding relative to each other, the produced tensile force ( $F_3$ ) should satisfy:

$$\bar{F}_1 < F_3 \ll \bar{F}_2 \tag{1}$$

where  $\bar{F}_1$  is the average of  $F_1$ , and  $\bar{F}_2$  is the average of  $F_2$ .

The force analysis was performed on one side of the clamped pepper, as shown in Figure 9.

The flexible end-effector was considered satisfactory if it did not slide relative to the pepper and was able to complete the harvesting action successfully:

$$\begin{cases} F_3 = f - G \\ f = \mu F_4 \\ F_4 < [\sigma]S \end{cases} \tag{2}$$

where  $\mu$  is the coefficient of friction between the flexible end-effector and the pepper, taking the value of 0.31;  $[\sigma]$  is the permissible stress of the horn pepper; and the allowable stress of  $[\sigma]$  is approximately 3.1 Mpa.



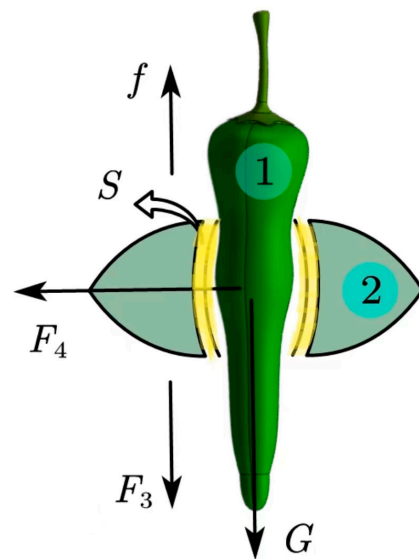


**Figure 9.** Force analysis of the pepper. In this diagram, 1 is the pepper; 2 is the flexible end-effector;  $G$  is the pepper weight, N;  $F_4$  is the horizontal clamping force applied by the flexible end-effector to the pepper, N;  $S$  is the contact area of the flexible end-effector with the pepper,  $\text{mm}^2$ ; and  $f$  is the friction created between the flexible end-effector and the pepper, N.

In addition, the designs of the geometric parameters of the flexible end-effector were carried out in this study, with the following considerations:

- The peppers were scattered throughout the pepper tree, so the flexible end-effector should be slender and shaped in a way that makes it easy to pick more deeply into the canopy [25];
- For maximum protection of the peppers, the clamping surface of the flexible end-effector should be larger, spreading out the average pressure during picking [26];
- To reduce manufacturing costs, the flexible end-effector structure should be as simple as possible [27];
- The design should meet the experimental prototype connection requirements:

$$\begin{cases} 7 < L < 8 \\ 1.5 < D < 2 \\ 280 < S < 320 \end{cases} \quad (3)$$

where  $L$  is the length of the flexible end-effector in the direction of the connection with the robot arm, cm;  $D$  is the thickness of the flexible end-effector in the direction perpendicular to  $L$ , cm; and  $S$  is the contact area of the flexible end with the pepper during operation,  $\text{mm}^2$ . Based on the appropriate  $L$  and  $D$  dimensions,  $S$  was determined by clamping experiments.

In summary, the four flexible end-effector model designs are shown in Figure 10.

### 3.3. Facility Agriculture Pepper-Picking Robot

In this study, the ROSMASTER X3 PLUS was selected as the mobile robotic arm platform, obtained from Shenzhen Yahboom Intelligent Technology Co. Ltd., Shenzhen, Guangdong Province, China. This platform is a wheel omnidirectional mobile robot developed based on an ROS robot operating system [28]. It is equipped with high-performance hardware configurations, such as LIDAR and a depth camera. It can perform robot motion control, map-building navigation, obstacle avoidance, auto driving, and other applications [29]. Therefore, this vehicle was used as the basis for designing the parameters of the flexible end-effectors and building the test prototype. The shape of the mobile robotic arm platform is shown in Figure 11.

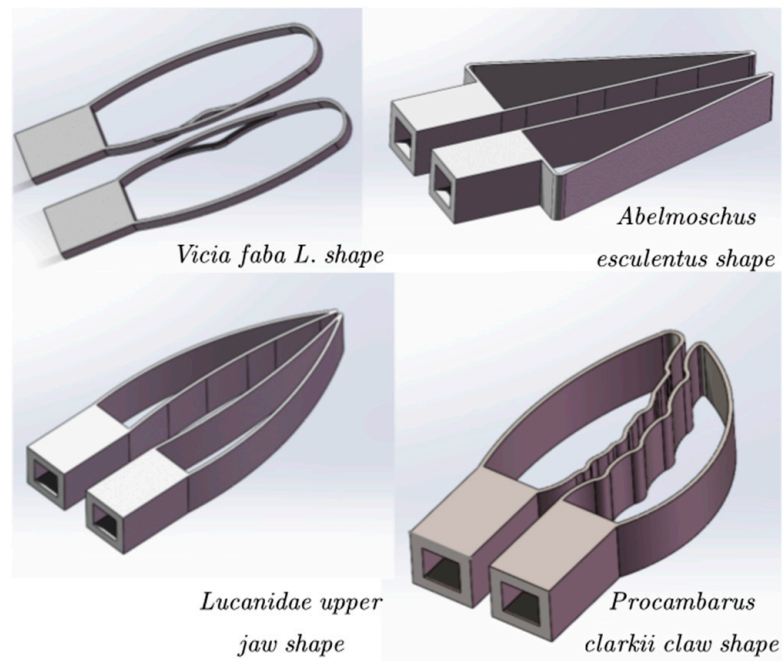


**Figure 10.** Four types of flexible end-effector model designs.



**Figure 11.** Mobile robotic arm platform profile.

The details of the computer used in this study are as follows: operating system: Ubuntu 18.04 LTS; CPU: Intel 8th generation Core i7 processor; RAM: 16 GB DDR4 memory; GPU: NVIDIA Quadro P3200 6 GB GDDR5 video memory, cuda version 10.0.1, cudnn version 10.0.1; and deep learning framework: pytorch1.2.0. The system framework of the experimental prototype consisted of a sensing module, a control unit, a motorized control module, a human-machine interaction module, and a power module. The system framework diagram of the experimental platform is shown in Figure 12.

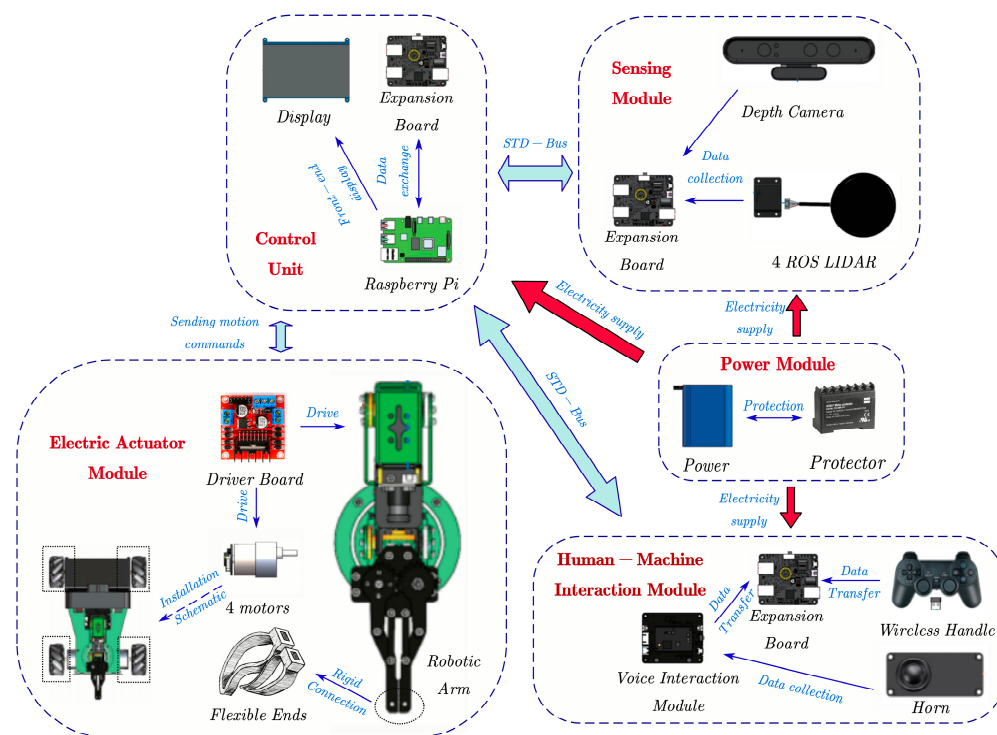


Figure 12. System framework diagram of the experimental platform.

The control unit was responsible for communication management, analyzing all information, and carrying out the logical operations; the sensing module was responsible for obtaining the three-dimensional spatial information of the peppers in the environment during the harvesting operations; the human–computer interaction module enabled the robot to understand human voice commands and accurately identify their intentions. This module enhanced the robot’s ability to accept commands during the experiments and reduced the difficulty in the operation of the pepper-harvesting robots in facility agriculture [30]. The power supply module provided electrical energy for all the links.

The working principle was based on the YOLOv5 target detection system, which utilized its deep feature extraction capabilities to accurately identify horn peppers. The system was further enhanced by incorporating the Astra Pro depth camera, enabling real-time pepper identification and positioning. The algorithms were utilized to calibrate both internal and external camera parameters, precisely extracting the target’s spatial three-dimensional coordinates for position determination. The identification and positioning system collected the spatial locations of the peppers, which were then transmitted to a Raspberry Pi for interpretation and instruction. The robot arm was controlled to execute specific movements of the flexible end-effector, such as gripping the pepper, swinging it up and down, and placing it into a basket, thus completing the picking process.

## 4. Feasibility and Optimization of Design

### 4.1. Structural Feasibility Verification

Due to the simple and dexterous design of the actuating end-effector of the robotic arm and its light overall mass, the main key structure for force and load bearing was the clamping linkage part, as displayed in Figure 13. Therefore, only the finite element simulation analysis of the clamping linkage was needed [31]. A clamping connecting rod component model was created in SolidWorks, and it was simplified following the principle of maintaining the accuracy of the analysis while reducing the calculation time. Features such as screw threads and chamfers, which do not significantly impact the results but do increase the computational load, were also simplified. The model of the clamping connecting rod can be seen in Figure 14.



Figure 13. Clamping linkage parts.

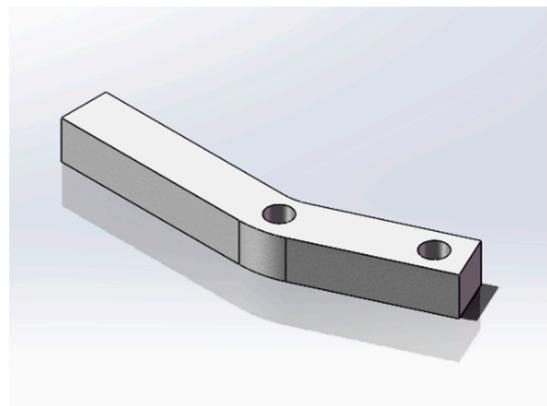


Figure 14. Model of clamping connecting rod component.

The material of the clamping connecting rod component was 1060 aluminum alloy, and the performance parameters are shown in Table 3. In this analysis, tetrahedral cells were selected for meshing, and a maximum cell length of 1.73 mm and a minimum edge length of 1.73 mm were obtained, for a total of 13,937 nodes and 8757 cells.

Table 3. Performance parameters of 1060 aluminum alloy.

Material	Modulus of Elasticity (N/mm <sup>2</sup> )	Poisson's Ratio	Density (g/cm <sup>3</sup> )	Permissible Stress (Mpa)
1060 aluminum alloy	69	0.33	2.78	126

According to the clamping rod components and the measurements of sample peppers, in which a 6 N pressure was applied, the corresponding constraints were applied to the two screw holes of the clamping rod components, which were then used for strain analysis and stress analysis. The deformation and maximum stress values were analyzed, and the stress–strain cloud diagrams of the clamping rod components are shown in Figure 15. If the structure meets the requirements, it should be consistent with the calibration formula [32]. The following are the results of the calibration formula:

$$S_{ca} = \frac{[\sigma_1]}{\sigma_1} \geq S_0 \quad (4)$$

where  $S_{ca}$  is the calculated safety factor;  $[\sigma_1]$  and  $\sigma_1$  are the permissible stress value and actual stress value, respectively, of the material, Mpa; and  $S_0$  is the standard safety factor.

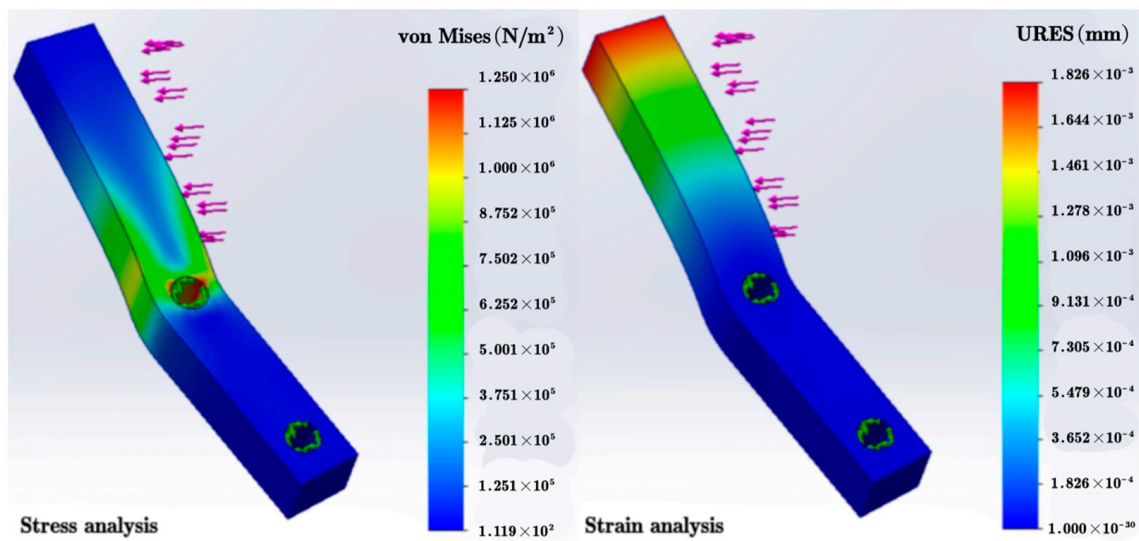


Figure 15. Stress–strain clouds of clamping connecting rod components.

The experimental data in Figure 15 show that when the clamping connecting rod part received 6 N of pressure, the maximum deformation was only 0.00182 mm, and the maximum stress was 1.250 MPa, taking the standard safety factor  $S = 1.5$ , which was still far lower than the permissible stress value of 1060 aluminum alloy,  $[\sigma] = 126$  MPa; thus, the structure of the clamping connecting rod part met the use requirements.

#### 4.2. Preliminary Determination of Optimal Design

In this study, an engineering plastic, namely, PLA plastic, was used for the lightweight design of a flexible end-effector structure. On the one hand, this material has suitable stiffness and strength and is a flexible material that can protect the skins of the peppers during the picking process [33]; on the other hand, PLA plastic is a general-purpose material suitable for 3D printing, which is economical and can be used to manufacture parts quickly and easily. The performance parameters of the PLA plastic are shown in Table 4.

Table 4. PLA plastic performance parameters.

Material	Modulus of Elasticity (N/mm <sup>2</sup> )	Poisson's Ratio	Density (g/cm <sup>3</sup> )	Permissible Stress (Mpa)
PLA plastic	2.7	0.351	1.10	24.5

Stress and strain in the structure can be predicted by performing a finite element analysis of the flexible end-effector [34]. In this study, we analyzed the stress distribution and deformation trends in four types of flexible end-effectors when holding peppers via the finite element method, optimized the design of each structure, and preliminarily determined the optimal design.

A pair of 4 N forces were applied according to the force conditions of pepper picking. The two forces were in opposite directions, the force area was the abdomen of each flexible end-effector's mating surface, and the specific force area varied slightly according to the shape of the flexible end-effector, which was approximately 328 mm<sup>2</sup>. The force area is shown in Figure 16. This part was the ideal working surface, which was able not only to provide suitable clamping force but also to ensure that the end-effector could be deformed enough to disperse the stress and protect the pepper. We added the corresponding constraints to the flexible end-effector, on the basis of which we performed strain and stress analyses for each of the four types of flexible end-effectors, and the deformation and maximum stress values of the overall structure were obtained after analyzing the data

and solving. The stress–strain cloud diagrams of the flexible end-effector are shown in Figure 17.

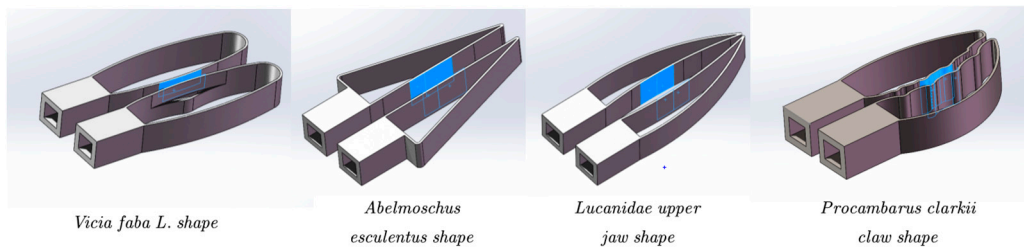


Figure 16. Stress areas.

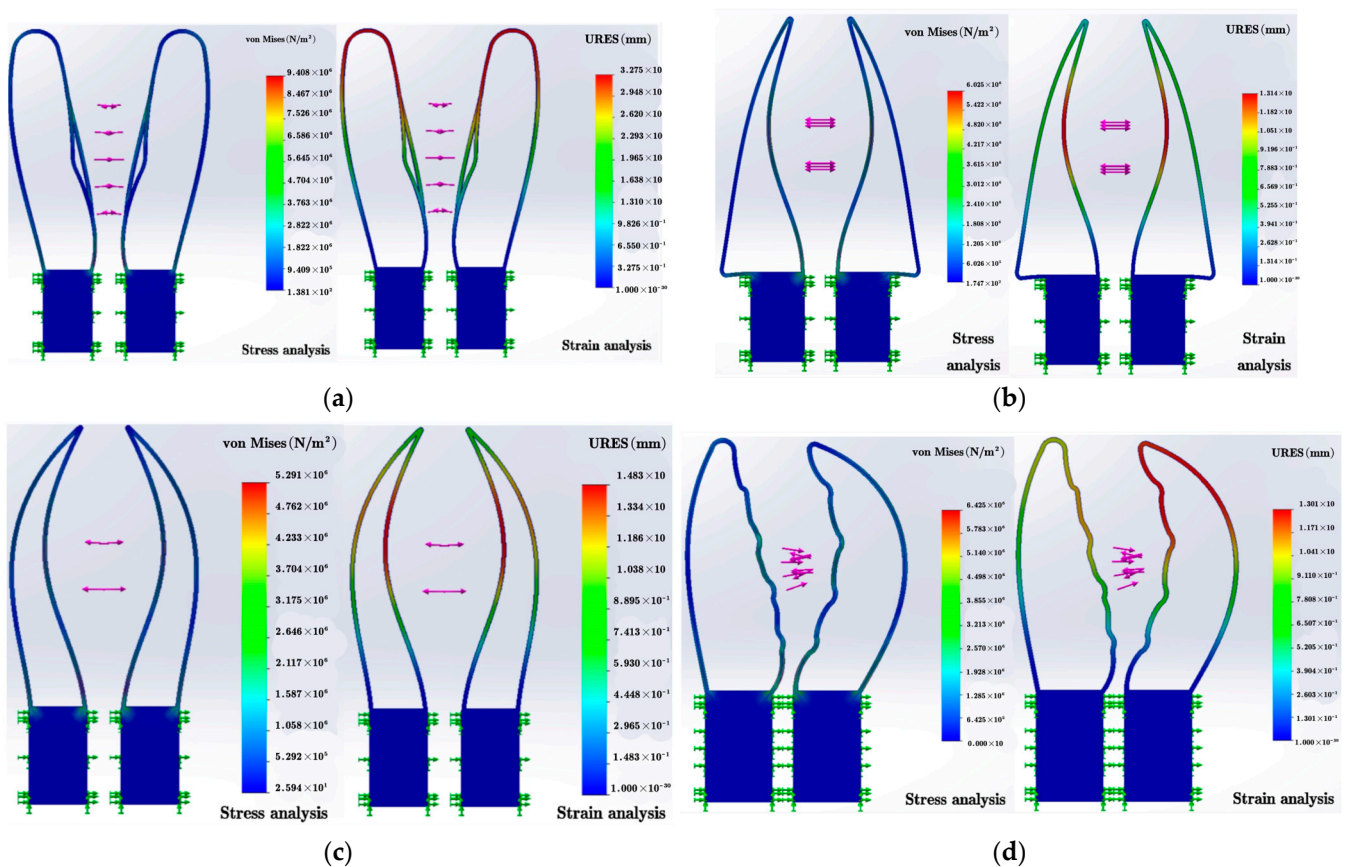


Figure 17. Stress–strain cloud diagrams of end-effectors of different shapes: (a) *Vicia faba L.*; (b) *Abelmoschus esculentus*; (c) *Lucanidae* upper jaw; and (d) *Procambarus clarkii* claw.

From the experimental data in Figure 17, it can be seen that the maximum stresses were observed when the four types of flexible end-effectors received 4 N of pressure, listed here in descending order: *Procambarus clarkii* claw shape, *Abelmoschus esculentus* shape, *Lucanidae* upper jaw shape, and *Vicia faba L.* shape. The maximum stress on the crayfish claw shape was 9.408 MPa, whereas the maximum stress on the broad bean fruit outer contour shape was 5.291 MPa. These results suggested that the broad bean fruit's outer contour shape exhibited a superior clamping ability compared with the other three bionic features, showcasing its better performance in clamping. As  $S = 1.5$ , both still had stress values lower than the permissible stress value for the PLA material  $[\sigma]$ . Considering the standard safety factor to be 24.5 MPa, the four flexible end-effector structure designs met the use requirements. In descending order, the strain of the four flexible end-effectors were the *Vicia faba L.* shape, the *Lucanidae* upper jaw shape, the *Abelmoschus esculentus* shape, and

the *Procambarus clarkii* claw shape. The largest value of the strain for the *Vicia faba* L. shape was 3.275 mm, which was presumed to have better wrapping ability compared with the other three shapes.

Taken together, it can be preliminarily judged that the design of the outer contour shape of the broad bean fruit was superior to the other three bionic feature designs via the finite element analysis method.

## 5. Field Trials

### 5.1. Experimental Conditions and Setting

In order to verify further the picking ability of the flexible end-effectors, a field trial was conducted in July 2023 at the pepper research base of Hunan Agricultural University, Changsha, Hunan Province, China. The peppers were cultivated according to the pot cultivation technique, the variety of the peppers was Hunan Research No. 15, the distance between the planting pots was 51 cm, the height was 23 cm, and the spacing between the longs was 182 cm. The experiment was conducted on a randomly selected line of pepper trees. The plants were more uniformly distributed, with an average height of approximately 83 cm, and the average water content of the fruit was 82% with a high fruiting rate. The terrain was flat with no evident potholes. The harvest trial site is shown in Figure 18.



**Figure 18.** Harvesting trial site.

In order to test the comprehensive picking performance of the facility agriculture pepper-picking robot in the natural environment, the adaptability of the picking robot was evaluated in various aspects. The test method used was “picking–evaluation–changing claw”. The picking robot picked rows of pepper trees and placed the harvested peppers in the designated baskets. Twenty peppers were picked for each flexible end, which was carried out six times in total. At the completion of each test, the work was paused for an overall assessment of the picked peppers and for a claw replacement; the order of replacement of the various claw shapes was *Vicia faba* L., *Abelmoschus esculentus*, *Procambarus clarkii* claw, and *Lucanidae* upper jaw. During each picking, the pepper picking robot adjusted the site of the flexible end grip based on the length and spatial location of the target pepper. The region of the chili pepper about 2/3 up from the low end of the fruit was harder, which was the ideal gripping site.

The picking experiment was officially started when the flexible end was first clamped onto a pepper. The following conditions were considered as broken peppers: (1) Pepper surface cracked or evidently deformed; (2) pepper fruit stalks mutilated or broken; and (3) causing other peppers to break during the picking process. All of the following were considered to be dropped peppers: (1) the flexible end was detached from the pepper

during the separation process; (2) the flexible end was unsuccessful in separating the pepper from the tree; (3) the pepper was dropped during transportation of the pepper to the collection basin; and (4) the separation process resulted in other peppers being dropped. The robot–work display interface is shown in Figure 19. The flexible end-effector picking shapes are shown in Figure 20.

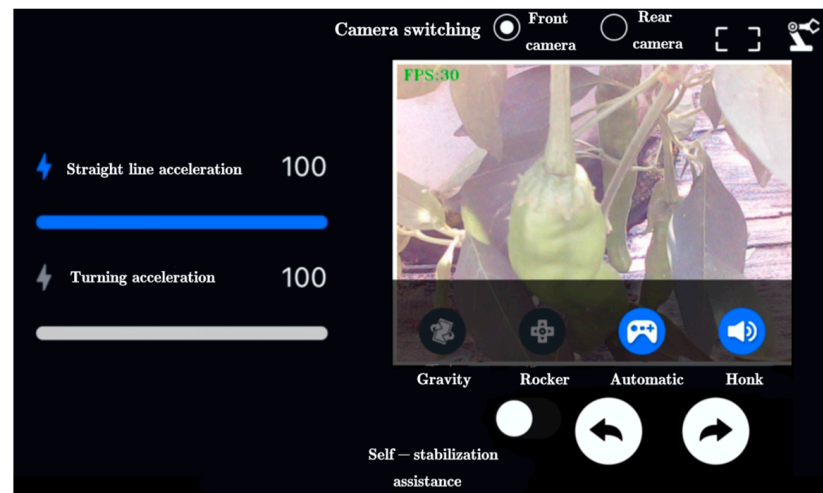


Figure 19. Picking experiment site, robot–work display interface.

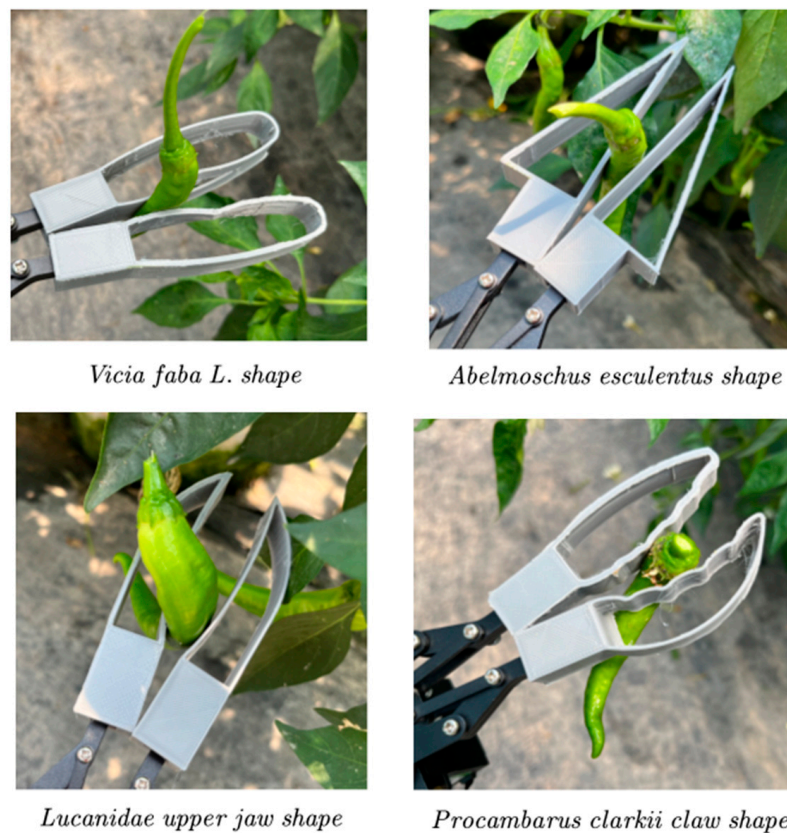


Figure 20. Display of various shapes of flexible end-effectors during picking.

## 5.2. Results and Discussion

The experiment was timed with a stopwatch. The evaluation indexes included the degree of breakage and the number of dropped fruits, which corresponded to the matching degree of the flexible end-effector of the bionic feature and the gripping ability, respectively.



The experimental data on breakage rates are shown in Table 5. The experimental data on drop rates are shown in Table 6.

**Table 5.** The experimental data on breakage rates.

Serial Number End-Effector Shape	1	2	3	4	5	6	Average Value	Average Breakage Rates (%)
The <i>Vicia faba</i> L. fruit	0	0	1	0	0	1	0.33	1.7
The <i>Abelmoschus esculentus</i> fruit	2	1	1	0	2	1	1.17	5.8
The upper jaw of a <i>Lucanidae</i>	1	0	2	0	1	1	0.83	4.2
The <i>Procambarus clarkii</i> claw	2	3	0	1	1	2	1.50	7.5

Twenty peppers were picked for each flexible end, which was carried out six times in total.

**Table 6.** The experimental data on drop rates.

Serial Number End-Effector Shape	1	2	3	4	5	6	Average Value	Average Drop Rates (%)
The <i>Vicia faba</i> L. fruit	0	1	2	0	0	1	0.67	3.3
The <i>Abelmoschus esculentus</i> fruit	2	1	1	0	2	3	1.50	7.5
The upper jaw of a <i>Lucanidae</i>	1	0	2	1	3	1	1.33	6.7
The <i>Procambarus clarkii</i> claw	2	0	1	1	2	3	1.50	7.5

Twenty peppers were picked for each flexible end, which was carried out six times in total.

As can be seen from Table 5, the breakage rates under the various shape designs, in order from best to worst, were *Vicia faba* L., *Procambarus clarkii* claw, *Abelmoschus esculentus*, and *Lucanidae* upper jaw. The *Vicia faba* L. flexible end-effector had the lowest average breakage rate. For 120 peppers picked, the average breakage rate was 1.7%. This meant that it had a better wrapping ability compared to the other three. As can be seen from Table 6, the drop rates, in order from best to worst, were *Vicia faba* L., *Procambarus clarkia* claw, *Abelmoschus esculentus*, and *Lucanidae* upper jaw shape. The *Vicia faba* L. flexible end-effector had the lowest average drop rate. The average drop rate was 3.3%. This meant that it had more clamping power compared to the other three products. In summary, the *Vicia faba* L. flexible end-effector had the strongest comprehensive picking ability, with the lowest fruit-breakage rate and drop rate, and it could well meet the operational requirements of pepper picking in facility agriculture. Twenty peppers were picked for each flexible end, which was carried out six times in total.

## 6. Conclusions

This paper focused on the characteristics of horn pepper varieties and presented a proposed design of a bionic-feature pepper flexible end-effector that yielded better results. Four biological features, namely, the outer contours of a broad bean fruit, okra epidermis, a stag beetle upper jaw, and a crayfish shrimp pincer, were carefully selected. The design process involved using SolidWorks to create the mimetic structure. To assess the feasibility of the four types of structures, finite element analysis was conducted on the strength and deformation of the flexible end-effector under various picking scenarios. Based on the analysis, the design imitating the broad bean fruit contour characteristics was identified as the optimal choice for the bionic-feature pepper flexible end-effector. Tensile experiments were performed to determine the pepper's resistance to validate the rationality of the picking program. The flexible end-effector was made via 3D printing technology. The print material was PLA plastic. The test prototype was built using the mobile robotic arm platform ROSMASTER X3 PLUS. By conducting field trials, the pepper-picking abilities

of the flexible end-effectors featuring different bionic characteristics were compared and analyzed. In six experiments, each flexible end was harvested for 120 horn peppers. The *Vicia faba* L. flexible end-effector had the lowest average breakage rate. The average breakage rate was 1.7%. The *Vicia faba* L. flexible end-effector had the lowest average drop rate. The average drop rate was 3.3%. The results indicated that the flexible end-effector designed to imitate the outer contour of a fava bean demonstrated the best performance. It exhibited a high work efficiency and significantly reduced the fruit-breakage and dropping rates, surpassing both the manual and traditional machine picking methods. As such, this bionic end-effector was found to be well suited to meet the operational demands of pepper picking in facility agriculture. It could reduce the amount of manual handling, complete harvesting tasks in less time, and save labor costs. This is especially important for facility agriculture where labor is expensive; using a suitable flexible end, robotic harvesting can minimize damage to the crop. This can increase yield and quality and improve the sustainability of facility agriculture; at the same time, we designed this small pepper-harvesting robot with a low threshold of input use, which was very suitable for the promotion of application. It can help more small- and medium-scale facility farms to mechanize, improve efficiency, and reduce costs. It can serve as a reference for the design of pepper-picking equipment in facility agriculture in the future.

It was found during this experiment that the production material of the flexible end-effector was an important factor affecting picking effectiveness, and the selection of a flexible material with a better wrapping effect on the clamped pepper not only reduced the falling rate but also effectively protected the pepper. Our research team will carry out in-depth research on the production material of the flexible end-effector.

Based on our testing of the mobile robotic arm platform ROSMASTER X3 PLUS, the picking flexible end-effector needs to be matched with excellent pepper-recognition technology to take full advantage of its role in the process. Next, our research team will carry out in-depth research on pepper recognition and the robotic arm to strive for further improvements.

In this study, a flexible end-effector was designed to be suitable for the harvesting of horn pepper varieties, and the benefits of this research will be expanded upon in the future by applying the investigation of this flexible end-effector for the harvesting of different pepper shapes.

**Author Contributions:** Conceptualization, T.L.; methodology, T.L. and L.D.; software, L.D., Y.H. and A.Q.; validation, L.D., Y.H. and A.Q.; formal analysis, L.D. and Y.H.; investigation, L.D. and Y.L.; resources, T.L.; data curation, L.D.; writing—original draft preparation, L.D., M.Y. and Y.L.; writing—review and editing, T.L., L.D. and A.Q.; visualization, L.D. and X.D.; supervision, T.L. and P.J.; project administration, T.L. and P.J.; funding acquisition, T.L. and P.J. All authors have read and agreed to the published version of the manuscript.

**Funding:** This research was funded by the Hunan Agricultural Machinery Equipment and Technological Innovation R&D Project (Xiang Cai Nong Zhi (2020) No. 107), the National Key R&D Program (No. 2022YFD2002001), the Hunan Agricultural University Student Innovation and Entrepreneurship Training Program (No. XCX2023115), Hunan Provincial Department of Education Scientific Research Project (No. 22C0079).

**Data Availability Statement:** Not applicable.

**Acknowledgments:** We give special thanks to Ke Huang from the College of Horticulture, Hunan Agricultural University, for providing the test site and test materials. We thank Huiping Huang from the College of Horticulture, Hunan Agricultural University, for her assistance in the experiment.

**Conflicts of Interest:** The authors declare no conflict of interest.

## References

1. Yu, J.; You, F.; Wang, J.; Wang, Z. Evolution Modes of Pepper Industry Clusters under the Perspective of Social Network—An Example from Xinfu District, Xinzhou, Shanxi Province. *Sustainability* **2023**, *15*, 4948. [\[CrossRef\]](#)
2. Abbasi, R.; Martinez, P.; Ahmad, R. The digitization of agricultural industry—a systematic literature review on agriculture 4.0. *Smart Agric. Technol.* **2022**, *2*, 100042. [\[CrossRef\]](#)
3. Cai, P.; Zhang, S. Research Status and Development Trend of Intelligent Mechanized Pepper Harvesting. *Asian J. Res. Crop Sci.* **2022**, *7*, 33–41.
4. Kootstra, G.; Wang, X.; Blok, P.M.; Hemming, J.; Van Henten, E. Selective harvesting robotics: Current research, trends, and future directions. *Curr. Robot. Rep.* **2021**, *2*, 95–104. [\[CrossRef\]](#)
5. Ren, K.; Yu, J. Research status of bionic amphibious robots: A review. *Ocean Eng.* **2021**, *227*, 108862. [\[CrossRef\]](#)
6. Li, J.; Luan, Z.; Wang, Y.; Huang, M.; Yan, J.; Wang, Y. Analysis modeling and experiment of bionic winding soft actuator inspired by plant tendrils. *Smart Mater. Struct.* **2023**, *32*, 35023. [\[CrossRef\]](#)
7. Akter, A.Y.; Basak, H. Design and analysis of biomimetics based excavator bucket and tooth. *Proc. Inst. Mech. Eng. Part E J. Process Mech. Eng.* **2022**, *236*, 1167–1175. [\[CrossRef\]](#)
8. Jiang, H.; Han, X.; Jing, Y.; Guo, N.; Wan, F.; Song, C. Rigid–Soft Interactive Design of a Lobster-Inspired Finger Surface for Enhanced Grasping Underwater. *Front. Robot. AI* **2021**, *8*, 787187. [\[CrossRef\]](#)
9. Hu, F.; Lyu, L.; He, Y. A 3D printed paper-based thermally driven soft robotic gripper inspired by cabbage. *Int. J. Precis. Eng. Manuf.* **2019**, *20*, 1915–1928. [\[CrossRef\]](#)
10. Bachche, S.; Oka, K. Design, modeling and performance testing of end-effector for sweet pepper harvesting robot hand. *J. Robot. Mechatron.* **2013**, *25*, 705–717. [\[CrossRef\]](#)
11. Arad, B.; Balendonck, J.; Barth, R.; Ben Shahar, O.; Edan, Y.; Hellström, T.; Hemming, J.; Kurtser, P.; Ringdahl, O.; Tielen, T. Development of a sweet pepper harvesting robot. *J. Field Robot.* **2020**, *37*, 1027–1039. [\[CrossRef\]](#)
12. Bac, C.W.; Hemming, J.; Van Tuijl, B.; Barth, R.; Wais, E.; van Henten, E.J. Performance evaluation of a harvesting robot for sweet pepper. *J. Field Robot.* **2017**, *34*, 1123–1139. [\[CrossRef\]](#)
13. Montoya-Cavero, L.; de León Torres, R.D.; Gómez-Espinosa, A.; Cabello, J.A.E. Vision systems for harvesting robots: Produce detection and localization. *Comput. Electron. Agr.* **2022**, *192*, 106562. [\[CrossRef\]](#)
14. Jin, L.; Xinyan, Q.; Chen, Y. Design and analysis on key components of a novel pepper harvester’s picking device. *Open Mech. Eng. J.* **2015**, *9*, 540–545. [\[CrossRef\]](#)
15. Wang, Y.; Deng, X.; Luo, J.; Li, B.; Xiao, S. Cross-task feature enhancement strategy in multi-task learning for harvesting Sichuan pepper. *Comput. Electron. Agric.* **2023**, *207*, 107726. [\[CrossRef\]](#)
16. Hespeler, S.C.; Nemati, H.; Dehghan-Niri, E. Non-destructive thermal imaging for object detection via advanced deep learning for robotic inspection and harvesting of peppers. *Artif. Intell. Agric.* **2021**, *5*, 102–117. [\[CrossRef\]](#)
17. Ning, Z.; Luo, L.; Ding, X.; Dong, Z.; Yang, B.; Cai, J.; Chen, W.; Lu, Q. Recognition of sweet peppers and planning the robotic picking sequence in high-density orchards. *Comput. Electron. Agric.* **2022**, *196*, 106878. [\[CrossRef\]](#)
18. Liu, T.; Ma, Y.; Yang, W.; Ji, W.; Wang, R.; Jiang, P. Spatial-temporal interaction learning based two-stream network for action recognition. *Inf. Sci.* **2022**, *606*, 864–876. [\[CrossRef\]](#)
19. Deng, L.; Liu, T.; Jiang, P.; Xie, F.; Zhou, J.; Yang, W.; Qi, A. Design of an Adaptive Algorithm for Feeding Volume–Traveling Speed Coupling Systems of Rice Harvesters in Southern China. *Appl. Sci.* **2023**, *13*, 4876. [\[CrossRef\]](#)
20. Li, B.; Lecourt, J.; Bishop, G. Advances in non-destructive early assessment of fruit ripeness towards defining optimal time of harvest and yield prediction—A review. *Plants* **2018**, *7*, 3. [\[CrossRef\]](#)
21. Li, W.; Pei, Y.; Zhang, C.; Kottapalli, A.G.P. Bioinspired designs and biomimetic applications of triboelectric nanogenerators. *Nano Energy* **2021**, *84*, 105865. [\[CrossRef\]](#)
22. Shahrubudin, N.; Lee, T.C.; Ramlan, R. An overview on 3D printing technology: Technological, materials, and applications. *Procedia Manuf.* **2019**, *35*, 1286–1296. [\[CrossRef\]](#)
23. Whenish, R.; Antony, M.M.; Balaji, T.; Selvam, A.; Ramprasath, L.S.; Velu, R. Design and performance of additively manufactured lightweight bionic hand. In Proceedings of the 3rd International Conference on “Advancements in Aeromechanical Materials for Manufacturing”: ICAAMM-2020, Hyderabad, India, 24–25 July 2020; AIP Publishing: New York, NY, USA, 2021.
24. Maskey, B.; Bhattarai, R.; Bhattarai, G.; Shrestha, N.K. Post-harvest quality of fresh akabare chili (*Capsicum chinense*) as affected by hydrocooling, package modification and storage temperature. *Int. J. Food Prop.* **2021**, *24*, 163–173. [\[CrossRef\]](#)
25. Huang, C.; Mees, O.; Zeng, A.; Burgard, W. Visual language maps for robot navigation. In Proceedings of the 2023 IEEE International Conference on Robotics and Automation (ICRA), London, UK, 29 May–2 June 2023; IEEE: New York, NY, USA, 2023.
26. Elsis, M.; Zaini, H.G.; Mahmoud, K.; Bergies, S.; Ghoneim, S.S. Improvement of trajectory tracking by robot manipulator based on a new co-operative optimization algorithm. *Mathematics* **2021**, *9*, 3231. [\[CrossRef\]](#)
27. Yang, Y.; Shi, J.; Liu, Z.; Liu, S. Vibration and position tracking control for a flexible Timoshenko robot arm with disturbance rejection mechanism. *Assem. Autom.* **2022**, *42*, 248–257. [\[CrossRef\]](#)
28. Mello, R.C.; Scheidegger, W.M.; Múnera, M.C.; Cifuentes, C.A.; Ribeiro, M.R.; Frizera-Neto, A. The PoundCloud framework for ROS-based cloud robotics: Case studies on autonomous navigation and human–robot interaction. *Robot. Auton. Syst.* **2022**, *150*, 103981. [\[CrossRef\]](#)

29. Varlamis, I.; Kontopoulos, I.; Tserpes, K.; Etemad, M.; Soares, A.; Matwin, S. Building navigation networks from multi-vessel trajectory data. *Geoinformatica* **2021**, *25*, 69–97. [[CrossRef](#)]
30. Pan, S. Design of intelligent robot control system based on human–computer interaction. *Int. J. Syst. Assur. Eng. Manag.* **2023**, *14*, 558–567. [[CrossRef](#)]
31. Lewis, G.S.; Mischler, D.; Wee, H.; Reid, J.S.; Varga, P. Finite element analysis of fracture fixation. *Curr. Osteoporos. Rep.* **2021**, *19*, 403–416. [[CrossRef](#)]
32. Gyurkó, Z.; Nemes, R. Aspects of size effect on discrete element modeling of concrete. *Pollack Period.* **2022**, *17*, 36–42. [[CrossRef](#)]
33. Gomez, E.F.; Wanasinghe, S.V.; Flynn, A.E.; Dodo, O.J.; Sparks, J.L.; Baldwin, L.A.; Tabor, C.E.; Durstock, M.F.; Konkolewicz, D.; Thrasher, C.J. 3D-printed self-healing elastomers for modular soft robotics. *ACS Appl. Mater. Interfaces* **2021**, *13*, 28870–28877. [[CrossRef](#)] [[PubMed](#)]
34. Bagha, A.K.; Bahl, S. Finite element analysis of VGCF/pp reinforced square representative volume element to predict its mechanical properties for different loadings. *Mater. Today Proc.* **2021**, *39*, 54–59. [[CrossRef](#)]

**Disclaimer/Publisher’s Note:** The statements, opinions and data contained in all publications are solely those of the individual author(s) and contributor(s) and not of MDPI and/or the editor(s). MDPI and/or the editor(s) disclaim responsibility for any injury to people or property resulting from any ideas, methods, instructions or products referred to in the content.